Atomic size effects on local coordination and medium-range order in molten trivalent metal chlorides

1992 J. Phys.: Condens. Matter 4 8933

(http://iopscience.iop.org/0953-8984/4/46/001)

J. Phys.: Condens. Matter 4 (1992) 8933–8944. Printed in the UK

Atomic size effects on local coordination and medium-range order in molten trivalent metal chlorides

H Tatlipinar†, Z Akdeniz†‡, G Pastore§ and M P Tosi||

† International Centre for Theoretical Physics, I-34014 Trieste, Italy
‡ Department of Physics of the University of Istanbul, Istanbul, Turkey
§ Department of Theoretical Physics of the University of Trieste, I-34014 Trieste, Italy
|| Scuola Normale Superiore, I-56100 Pisa, Italy

Received 20 August 1992

Abstract. Structural correlations in molten trivalent metal chlorides are evaluated as functions of the metal ion size R_M across the range from $LaCl_3$($R_M \approx 1.4$ Å) to $AlCl_3$ ($R_M \approx 0.8$ Å), using a charged soft-sphere model and the hypernetted chain approximation. Main attention is given to trends in the local liquid structure (partial radial distribution functions, coordination numbers and bond lengths) and in the intermediate-range order (first sharp diffraction peak in the number–number and partial structure factors). The trend towards fourfold local coordination of the metal ions, the stabilization of their first-neighbour chlorine cage and the growth of medium-range order are found to proceed in parallel as the size of the metal ion is allowed to decrease at constant number density and temperature. A tendency to molecular-type local structure and liquid–vapour phase separation is found within the hypernetted chain scheme at small metal ion sizes corresponding to $AlCl_3$ and is emphasized by decreasing the number density of the fluid. The predicted molecular units are rather strongly distorted Al_2Cl_6 dimers, in agreement with observation. The calculated structural trends for other trichlorides are compared with diffraction and transport data.

1. Introduction

Liquid structures studies of molten salts by neutron and x-ray diffraction have recently focused on trivalent metal halides. The available structural data, in combination with the measured melting parameters (volume and entropy change across melting) and transport coefficients (electric conductivity and shear viscosity of the melt) that are available for many trihalides, have led to a classification of melting mechanisms and liquid structure types for these systems [1, 2]. Focusing here on those trihalides that have been examined in diffraction experiments, the following trends in melting mechanism has been noticed:

(i) lanthanide metal trichlorides crystallizing in the typically ionic UCl_3 structure, such as $LaCl_3$, $PrCl_3$, $NdCl_3$, $SmCl_3$ and $GdCl_3$, melt with an appreciable volume change into fully ionized liquids [3];

(ii) YCl_3 melts with a very small volume change from the layer-type $AlCl_3$ structure into an ionic liquid which, through the presence of a first sharp diffraction peak (FSDP) in the neutron diffraction pattern at scattering wave number $k = 0.95$ Å^{-1}, shows intermediate-range order from octahedral-type coordination [4];

0953-8984/92/468933+12$07.50

(iii) $AlCl_3$ melts with large volume and entropy changes from the same layer structure into a slightly ionized liquid of molecular Al_2Cl_6 dimers, the ideal dimer consisting of two tetrahedrally coordinated Al^{3+} ions with a shared Cl–Cl edge (see [5] and references given therein);

(iv) $SbCl_3$ melts with an abnormally low entropy change from a molecular-type crystal structure into a slightly ionized liquid of molecular monomers with strong intermolecular correlations [6]. It has also been stressed [1] that these melting and structural behaviours correlate with an indicator of the character of the chemical bond measuring the chemical activity of the metallic element.

While a quantitative theoretical account of these melts from realistic models of the interionic forces or more basic descriptions of the chemical bond is still largely a challenge, the present work examines to what extent a standard ionic model involving coulombic interactions and soft-sphere overlap repulsions may help to provide a semiquantitative scenario for such structural and melting trends. The model that we adopt has already proved useful in regard to molten YCl_3 [7], by yielding approximate agreement with several features of the measured neutron diffraction pattern and by providing some insight into partial structure factors and radial distribution functions. As we shall see, the trends from (i) to (iii) above can indeed be reproduced by such a simple model in correlation with the size R_M of the metal ion and with the number density of the melt.

In essence, with decreasing R_M a charged soft-sphere model predicts an increasing stabilization of the first-neighbour chlorine shell of the metal ion, ending in a long-lived fourfold coordination in correspondence with $AlCl_3$ at high density. This trend in the local liquid structure favours connectivity of the melt over increasing distances, leading to intermediate-range order and to the attendant FSDP. Decreasing the number density favours the formation of bound molecular states. The stabilization of the coordination shell of the metal ion and the parallel growth of the FSDP are expected to be independent of the details of the interionic forces. However, the stabilization of molecular bound states is sensitive to the modelling of the interactions. In particular, the stability of a monomer in the shape of a trigonal pyramid with the metal ion at its apex, as is the case for $SbCl_3$, cannot be described without an explicit account of chemical bonding. This specific monomer shape is expected to be crucial for the strong intermolecular correlations that have been observed in molten $SbCl_3$ [8]. More generally, fully quantitative comparisons with the data would require, in addition to coulombic interactions and soft steric repulsions, an account of the large electronic polarizability of the chlorine ions and the inclusion of three-body forces accounting for covalent contributions to the bonding.

In so far as the main focus of the present work is on the role of steric effects combined with coulomb ordering in the melt, the even simpler model of charged hard spheres might have been adopted, as was done with similar purposes for the molten alkali halides [9]. This would present a definite advantage if the analytic solution given by the mean spherical approximation (MSA) could still be used for liquid structure. However, it is well known that the MSA yields radial distribution functions that are grossly in error at short range for charged hard spheres carrying appreciably different charges. We have consequently adopted the hypernetted chain approximation (HNC), which is quite accurate for ionic liquids and in particular guarantees positivity of the radial distribution functions at short range. Given the need for a numerical solution of the model, the adoption of soft spheres has the advantage that average bond

lengths can be precisely evaluated. A correspondence between size parameters and real systems is already available from calculations of ionic bonding for molecular-ion complexes in molten halide mixtures [10].

The layout of the paper is as follows. In section 2 we give a brief presentation of the model and discuss the choice of its parameters for the systems of present interest, spanning the range from $LaCl_3$ to $AlCl_3$. We also describe the solution of the model for liquid pair structure in the HNC. The calculated trends in liquid structure as a function of the metal ion size at fixed number density and temperature are presented and discussed in section 3, while in section 4 we illustrate the consequences of a sharp drop in number density for metal ion sizes in the range appropriate to $AlCl_3$. Finally, section 5 gives a brief summary and some concluding remarks.

2. The model and its solution

The pair potential $\Phi_{ij}(r)$ between ions of types i and j at separation r is taken as the sum of their coulombic interaction and a short-range overlap repulsion,

$$\Phi_{ij}(r) = Z_i Z_j e^2/r + f(\rho_i + \rho_j)\exp[(R_i + R_j - r)/(\rho_i + \rho_j)]. \quad (1)$$

This form, which goes back to the early work of Busing [11], describes each ion by a valence Z_i, an effective radius R_i and an effective hardness ρ_i. In our choice for the overlap parameters in equation (1) we have made use of the analysis given by Erbölükbas *et al* [10] for the bond lengths and the vibrational Raman frequencies of bound molecular-ion states formed by trivalent metal ions in liquid mixtures of their halides with alkali halides. The alkali halide component of the mixture acts as a halogen donor to yield molecular ions in a stable octahedral-type configuration both for lanthanide metal ions in chloride mixtures and for the Al ion in fluoride mixtures. Denoting the trivalent metal ion by the suffix M, we have adopted in our calculations the values $Z_M = 3$, $Z_{Cl} = -1$, $f = 0.05\ e^2\ \text{Å}^{-2}$, $R_{Cl} = 1.71$ Å, $\rho_{Cl} = 0.238$ Å and $\rho_M = 0.007$ Å. We have allowed R_M to vary in the range $0.82\ \text{Å} \leqslant R_M \leqslant 1.42\ \text{Å}$. Table 1 shows the relationship between specific values of R_M in this range and several trivalent metal ions.

Table 1. Values of the ionic radius R_M (in Å) for several trivalent metal ions (from [10]).

La^{3+}	Ce^{3+}	Pr^{3+}	Nd^{3+}	Sm^{3+}	Gd^{3+}	Dy^{3+}	Y^{3+}	Al^{3+}
1.44	1.41	1.38	1.36	1.30	1.26	1.22	1.20	0.82

With the above model interactions we have evaluated the partial pair distribution functions $g_{ij}(r)$ and the corresponding partial structure factors $S_{ij}(k)$,

$$S_{ij}(k) = \delta_{ij} + n(x_i x_j)^{1/2} \int \mathrm{d}\boldsymbol{r}\ [g_{ij}(r) - 1]\exp(\mathrm{i}\boldsymbol{k}\cdot\boldsymbol{r}). \quad (2)$$

In equation (2) n is the number density of formula units and x_i is the number of ions of type i in the formula unit. The calculations of liquid structure are based on the Ornstein–Zernike equations for the partial direct correlation functions $c_{ij}(r)$,

$$h_{ij}(r) = c_{ij}(r) + n\sum_l x_l \int \mathrm{d}\boldsymbol{r}'\ h_{il}(r')c_{lj}(|\boldsymbol{r} - \boldsymbol{r}'|) \quad (3)$$

where $h_{ij}(r) = g_{ij}(r) - 1$, in combination with the hypernetted chain closure,

$$g_{ij}(r) = \exp[-\Phi_{ij}(r)/(k_B T) + h_{ij}(r) - c_{ij}(r)]. \tag{4}$$

These equations have been solved numerically on a grid of 513 points by means of the algorithm developed by Gillan [12] and Abernethy and Gillan [13], with an r-spacing of 0.098 Å corresponding to a k-spacing of 0.063 Å^{-1}.

Other structural properties of present interest are the running coordination numbers $N_{ij}(r)$,

$$N_{ij}(r) = 4\pi n x_j \int_0^r g_{ij}(r') r'^2 \, dr'. \tag{5}$$

The coordination numbers that we shall report are defined as $2N_{ij}(d_{ij})$, where d_{ij} is the appropriate 'bond length', i.e. the position of the first peak in $g_{ij}(r)$. We shall also report average structure factors $S_{av}(k)$, defined by

$$S_{av}(k) = \left(\sum_i x_i b_i^2\right)^{-1} \left(\sum_{ij} (x_i x_j)^{1/2} b_i b_j S_{ij}(k)\right) \tag{6}$$

and the corresponding radial distribution functions $g_{av}(r)$,

$$g_{av}(r) = 1 + (2\pi^2 n r)^{-1} \int_0^\infty [S_{av}(k) - 1] \sin(kr) k \, dk. \tag{7}$$

Depending on the choice of the weight factors b_i, equations (6) and (7) yield either the neutron scattering or the x-ray scattering functions. The choice $b_i = 1$ yields the number–number structure factor.

3. Structural trends at constant density and temperature

In the calculations that we report in this section the number density and the temperature have been kept fixed at the values $n = 0.0316$ Å^{-3} and $T = 1020$ K. These values are appropriate to YCl_3 near freezing, this compound lying near the middle of the range of R_M that we examine. The calculated pressure at this density and temperature is nevertheless approximately constant over the range of R_M.

3.1. Local structure

The M–Cl radial distribution function at three values of R_M is shown in figure 1 as a function of distance r normalized to the average ion-sphere radius $a = (4\pi n/3)^{-1/3} = 1.96$ Å. Of course, the M–Cl bond length d decreases linearly with R_M, as is shown in the inset in figure 1. It is evident from the behaviour of the first-neighbour peak and of the subsequent minimum that the first-neighbour shell is being stabilized with decreasing R_M. This effect is brought out more clearly in figure 2, showing the M–Cl running coordination number as a function of r/a for five values of R_M. At $R_M = 1.42$ Å the number of chlorine first neigbours about a trivalent metal ion is of order 7 and there is appreciable exchange of chlorines between the first- and second-neighbour shells. The plateau in $N_{+-}(r)$ decreases in

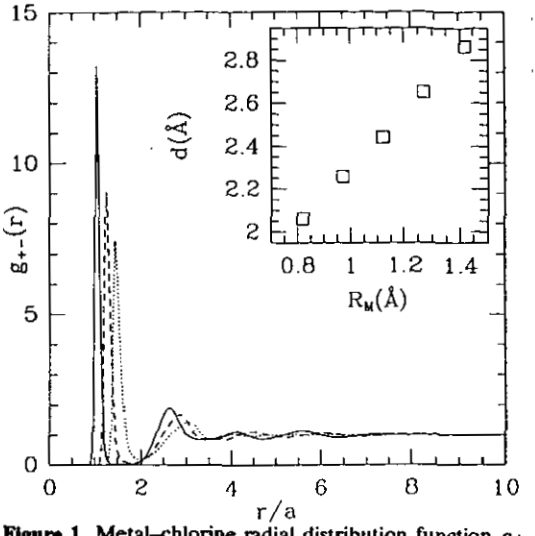

Figure 1. Metal–chlorine radial distribution function $g_{+-}(r)$ for $R_M = 1.42$ Å (a short-dashed curve), $R_M = 1.12$ Å (a long-dashed curve) and $R_M = 0.82$ Å (full curve). The inset shows the metal–chlorine bond length d (position of the main peak in $g_{+-}(r)$) as a function of R_M.

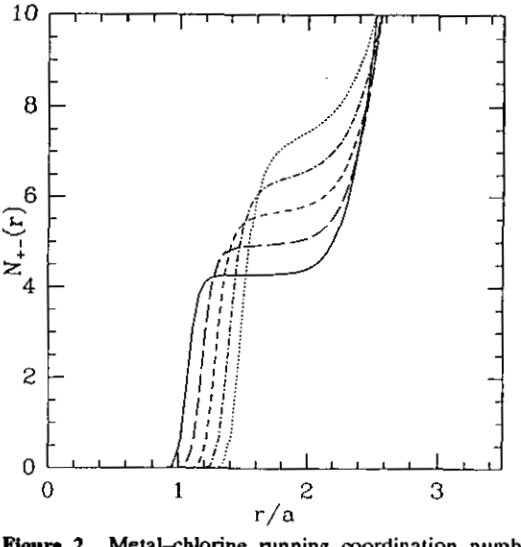

Figure 2. Metal–chlorine running coordination number $N_{+-}(r)$ for $R_M = 1.42$ Å, $R_M = 1.27$ Å, $R_M = 1.12$ Å, $R_M = 0.97$ Å and $R_M = 0.82$ Å(from top to bottom).

height and flattens out with decreasing R_M, until at the opposite end of the range of R_M ($R_M \approx 0.82$ Å) the number of chlorines about the trivalent metal ion reaches a value of about 4 and the exchange between the first-neighbour shell and the rest of the liquid is almost completely suppressed.

The structure that we obtain at $R_M = 0.82$ Å may be representative of $AlCl_3$ in a partly ionized state, as may be realized by an increase in temperature or by application of pressure (see for instance the discussion of slightly ionized molecular-type fluids given by Hensel [14]). Further hints on its local structure will be obtained below through a discussion of like-ion correlations. The local coordination of the metal ion appears to be of distorted tetrahedral type, as is indicated by the bond

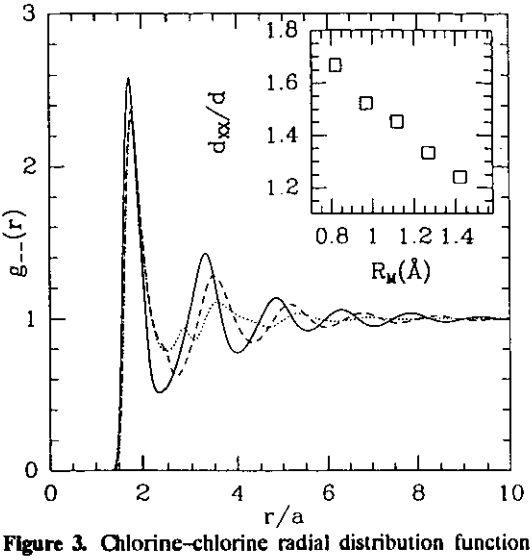

Figure 3. Chlorine–chlorine radial distribution function $g_{--}(r)$ at three values of R_M (symbols as in figure 1). The inset shows the chlorine–chlorine bond length, in units of the metal–chlorine bond length, as a function of R_M.

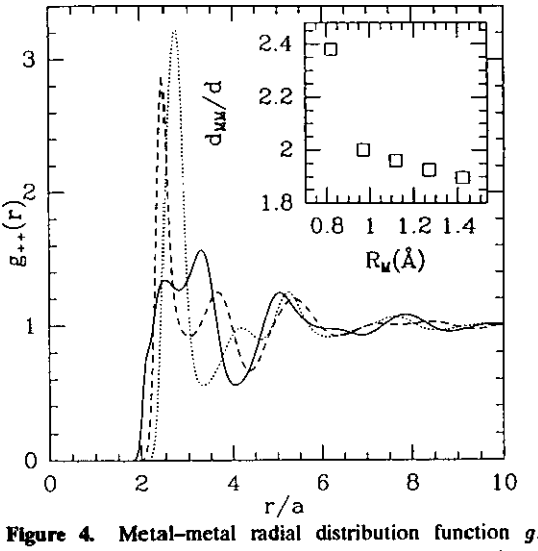

Figure 4. Metal–metal radial distribution function $g_{++}(r)$ at three values of R_M (symbols as in figure 1). The inset shows the metal–metal bond length, in units of the metal–chlorine bond length, as a function of R_M.

length for chlorine pairs. From the definition of the running coordination number for unlike-ion pairs given in equation (5), the number of trivalent metal ions about a chlorine is about $\frac{4}{3}$. The value $\frac{4}{3}$ is the one appropriate to chlorines in the Al_2Cl_6 dimer. However, the M–M bond length and the M–M coordination number are appreciably larger than would be appropriate to a simple fluid of ideal Al_2Cl_6 dimers. Thus, while several features of the local structure are reminiscent of the dimer, there certainly are very strong distortions and interconnections between local coordinations at the present fluid density.

Figures 3 and 4 report the Cl–Cl and M–M radial distribution functions for three values of R_M, with insets showing the ratios d_{XX}/d and d_{MM}/d between the bond lengths for like- and unlike-ion pairs. The chlorine–chlorine bond length is

approximately constant over the whole range of R_M and hence the ratio d_{XX}/d increases with decreasing R_M, to reach a value close to that appropriate for ideal tetrahedral coordination ($d_{XX}/d = (\frac{8}{3})^{1/2} = 1.633$) at $R_M \approx 0.8$ Å. This coordination will be further stabilized in real systems by chemical bonding.

In fact, the calculated chlorine–chlorine bond length increases rapidly by about 0.1 Å with increasing R_M in the narrow interval $R_M \approx 1 \div 1.1$ Å, whereas it is closely constant outside this interval. This change in d_{XX} preludes to changes in the detailed shape of $g_{--}(r)$ beyond close contact, which develop at larger R_M. The rearrangements in the relative distribution of chlorine pairs can be seen from the results for $g_{--}(r)$ in figure 3. The chlorine–chlorine coordination number, evaluated as specified in section 2 and therefore representing the number of chlorine pairs in near contact, is approximately equal to 5.4 throughout the whole range of R_M, except again in the neighbourhood of $R_M \approx 1$ Å where it dips somewhat below 5. The value appropriate to an isolated Al_2Cl_6 unit is $\frac{11}{3}$. Of course, further chlorine pairs in close contact would be present in a dense fluid of molecular dimers.

As is shown in figure 4, the changes in the M–M radial distribution function with R_M are much more drastic. Gross changes in $g_{++}(r)$ occur again in the neighbourhood of $R_M \approx 1$ Å. Below this value of R_M, neighbouring M–M pairs have a very broad distribution with an internal double-peak structure. This structure is a precursor to an instability of the homogeneous fluid state occurring, as we shall see in section 4, at appreciably lower densities and temperatures. While it is hard to obtain significant values for the M–M bond length and coordination number from such a broad distribution, from the first peak in the double structure we obtain $d_{MM}/d > d_{XX}/d$ (see insets in figures 3 and 4) and estimate an M–M coordination number of order 3. These values are in contrast with an interpretation of the calculated liquid structure at $R_M \approx 0.8$ Å as that appropriate to a simple fluid of ideal molecular dimers.

Above $R_M \approx 1$ Å, the structure in $g_{++}(r)$ is resolved into two separate peaks for first and second M–M neighbours, with the coordination number for M–M pairs in close contact increasing towards a value of order 8 at $R_M \approx 1.4$ Å. The M–M bond length increases slowly in this range and hence the d_{MM}/d ratio decreases slowly, as can be seen in the inset in figure 4.

3.2. *Short- and intermediate-range order*

Figures 5 and 6 report the number–number structure factor and the partial structure factors of the model liquid at three values of R_M. The number–number structure factor $S_{NN}(k)$ is especially significant in regard to the formation of order at intermediate range in the melt, which is signalled by the presence of a FSDP in this structural function at $k \approx 1$ Å^{-1} [15, 16]. It is evident from figure 5 that intermediate-range order is very strong at the lower end of the range of R_M and progressively weakens as R_M increases. This behaviour with ionic size parallels the decreasing stability shown for the local coordination structure of the metal ions in figure 2. A strong and stable local structure is clearly a prerequisite for the formation of the medium-range connectivity which is reflected in a prominent FSDP.

The detailed shape of $S_{NN}(k)$ at larger wave numbers reflects instead the nature of the short-range order in the melt. It is seen from figure 5 that the evolution of this structural function with R_M is very complex and we have to turn to the partial structure factors $S_{ij}(k)$ in figure 6 in order to understand it. At $R_M = 0.82$ Å the

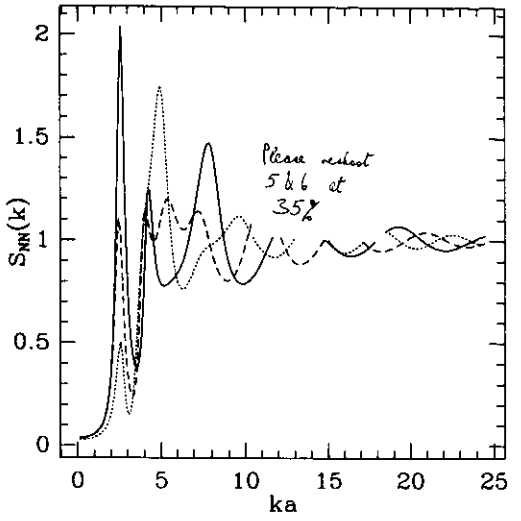

Figure 5. Number–number structure factor $S_{NN}(k)$ at three values of R_M (symbols as in figure 1).

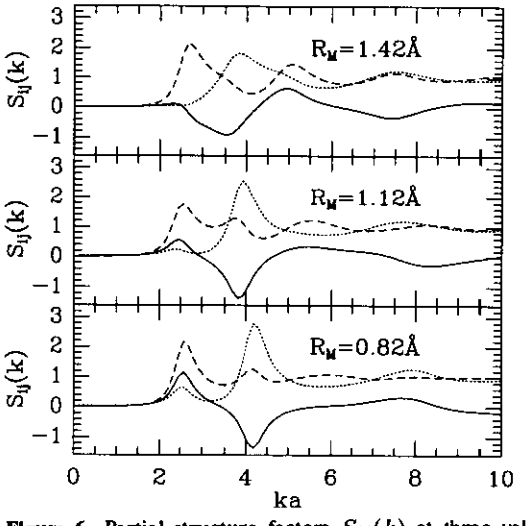

Figure 6. Partial structure factors $S_{ij}(k)$ at three values of R_M. Short-dashed curve: $S_{ClCl}(k)$; long-dashed curve: $S_{MM}(k)$; full curve: $S_{MCl}(k)$.

state of order in the melt is a simple combination of coulombic relative ordering of the components (peaks in $S_{MM}(k)$ and $S_{ClCl}(k)$ at $k \approx 2.1$ Å^{-1} in phase with a trough in $S_{MCl}(k)$) and intermediate-range ordering from connectivity of strong local structures (peaks in all the partial structure factors at $k \approx 1.2$ Å^{-1}, the most prominent one being that in the M–M structure factor). At $R_M = 1.42$ Å, on the other hand, the partial structure factors are qualitatively similar to those determined by neutron diffraction experiments on molten $SrCl_2$ [17]. The main ordering arises from the coulombic repulsion beween the polyvalent ions, leading to a main peak in $S_{MM}(k)$ which is appreciably higher and sharper than the main peak in $S_{ClCl}(k)$ and out of phase with it. $S_{MCl}(k)$ shows a main trough at an intermediate wave number between the positions of the main peaks in the like-ion structure factors. Coulombic relative ordering of the two components of the melt is still present, but is to some extent

frustrated by the dominant role of the repulsions between polyvalent ions. Clearly, the partial structure factors given in figure 6 at $R_M = 1.12$ Å show an intermediate stage in the evolution of ordering with ionic size, in which medium-range ordering and relative coulombic ordering coexist and are frustrating each other to some extent. It is worth noticing explicitly that the main peak in the M–M structure factor does not shift by any major amount during the evolution of the nature of ordering with ionic size.

3.3. Comparisons with experimental data

Figure 7 compares our results for the structure of MCl_3 melts in a charged soft-sphere model with experimental data on molten YCl_3 from neutron diffraction [4] and on molten $LaCl_3$ and $GdCl_3$ from x-ray diffraction [3]. The theoretical results have been obtained from equations (6) and (7) using weights given by standard neutron or x-ray scattering form factors. We only wish to stress the qualitative agreement between our results and experiment in regard to the structural evolution that is taking place from large values of R_M (La^{3+} and Gd^{3+}) to intermediate values of R_M (Y^{3+}). As was emphasized in section 1, fully quantitative comparisons between theory and experiment would require the development of more refined models for these melts. At the same time it would be of relevant interest to determine in more detail the structure of molten trihalides by the measurement of partial structure factors.

It is also interesting to notice that the stabilization of the first coordination shell with decreasing R_M, that was illustrated in figure 2, finds indirect confirmation in the available data for the ionic conductivity σ of trichlorides near freezing [2]. Over the range from $LaCl_3$ to YCl_3 σ decreases from 1.3 Ω^{-1} cm^{-1} to 0.4 Ω^{-1} cm^{-1}. The available data indicate that this change in σ is only partly due to the difference in melting temperature (1131 K for $LaCl_3$ and 994 K for YCl_3). Our earlier parallel between $LaCl_3$ and $SrCl_2$ is supported by comparison of their electric conductivities at freezing ($\sigma = 2.0$ Ω^{-1} cm^{-1} for $SrCl_2$ at 1146 K).

4. The role of liquid density and temperature

We have already pointed out that the values of the liquid density and temperature adopted in the calculations discussed in section 3 ($n = 0.0316$ Å^{-3} and $T = 1020$ K) are quite high compared to those of liquid $AlCl_3$ near freezing at standard pressure ($n = 0.0234$ Å^{-3} and $T = 466$ K). The local liquid structure calculated there for $R_M = 0.82$ Å, though showing some features that are reminiscent of a dense fluid of Al_2Cl_6 dimers, is characterized by an M–M radial distribution function which is in contrast with this possibility. We explore in the present section the consequences of reducing the density and the temperature of our model fluid at $R_M = 0.82$ Å.

It should be emphasized that both the choice of the model and the choice of the statistical mechanical approximation have important consequences in a search for the formation of molecular bound states in a dense fluid matrix. Very crudely, the lack of chemical bonding and halogen polarizability in our model may be compensated by examining its behaviour at somewhat lower densities than the real one given above for liquid $AlCl_3$. One may expect that an artificial depression in density would help the formation of molecular bound states by purely coulombic interactions between the components, even though the binding energy of a molecular unit may be underestimated by perhaps 10% in the present case. In addition, there is no *a priori*

assurance that the HNC scheme is sufficiently accurate for quantitative predictions on such a structural transition in the liquid state. Bearing these limitations in mind, we illustrate below the role of density and temperature by reporting on calculations in which n has been arbitrarily fixed at half the density of liquid $AlCl_3$ and the temperature is lowered from $T = 1020$ K.

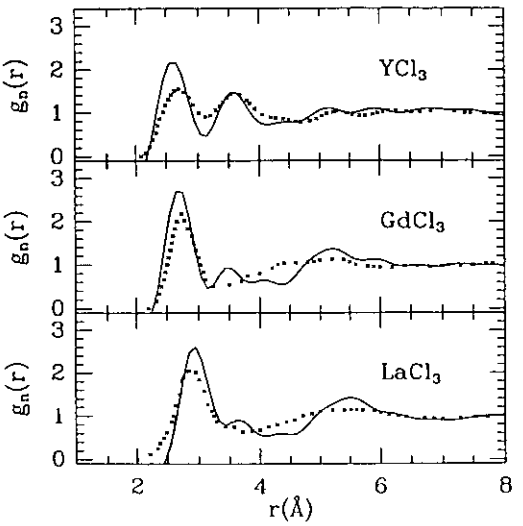

Figure 7. Theoretical results for the neutron scattering pair distribution function of molten YCl_3 and for the x-ray scattering pair distribution functions of molten $GdCl_3$ and $LaCl_3$, compared with experimental data from [4] and [3].

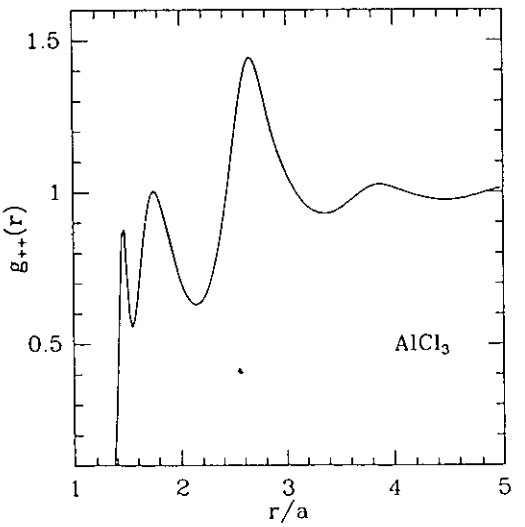

Figure 8. Metal–metal radial distribution function $g_{++}(r)$ for $R_M = 0.82$ Å at $n = 0.0117$ Å^{-3} and $T = 1020$ K.

We find that the decrease in density further strengthens the stability of the first-neighbour shell, leaving an essentially fourfold coordination of the trivalent ions by chlorines of distorted tetrahedral type. It also reduces the Cl–Cl coordination number to a value slightly below 4 and induces major changes in the M–M radial distribution

function, as is shown in figure 8 at $T = 1020$ K. The double-peak structure shown by $g_{++}(r)$ in figure 4 is resolved into two separate peaks, which are shifted to appreciably lower distance. The bond-length ratio d_{MM}/d thus approaches the d_{XX}/d ratio, although it still is somewhat larger. The M–M coordination number obtained by integration over *both* peaks is approximately unity. Intermediate-range order is still present in the partial structure factors.

Clearly, the decrease in density strengthens the resemblance of local structure in the model fluid to that of a fluid of Al_2Cl_6 dimers. The model fluid at the present density appears to be composed of distorted dimers, the distortion from the ideal shape of the dimer being undoubtedly emphasized by the oversimplified nature of the model. In particular, the overestimate of the d_{MM} bond length indicates that the dimer is elongated in the model by the unscreened coulombic repulsion of the two metal ions. In the real dimer this repulsion is screened by the polarization of the halogens, and the ideal shape of an edge-sharing double tetrahedron is stabilized by covalent contributions to the binding. Two possible distorted configurations for the dimer are suggested within the model by the double-peak structure shown in figure 8.

A decrease in temperature does not induce further major changes in the local structure, but drives the partial structure factors for $k \to 0$ towards a divergence occurring at $T \approx 520$ K. This behaviour signals an instability of the homogeneous fluid phase against phase separation into two phases of different density. Namely, at the arbitrarily chosen density $n = 0.0117$ Å^{-3} and at $T \approx 520$ K, the solution of the model in the HNC meets the spinodal curve for liquid–vapour phase separation.

5. Summary and concluding remarks

Our calculations have focused on the ionic radius of the metal ions as a very relevant (though not exclusive) parameter in determining the melting mechanism and the type of liquid structure for trivalent metal halides. The main result has been to demonstrate the correlation that exists between the formation of a strong local coordination and the growth of intermediate-range order in the liquid. The latter may be induced by strong interactions between local molecular-like coordinations in a dense liquid and is not necessarily associated with a covalent network structure of the liquid.

The detailed scenario that we have built by allowing the metal ion size to change over the range from La^{3+} to Al^{3+} is in full agreement with the observed trends that we have summarized in the introductory section. Covalent contributions to the bonding would modify the details and presumably sharpen the transitions between different types of liquid structure, but the overall picture that we have obtained in a simple ionic model appears to be essentially correct.

At the upper end of the range of R_M that we have examined, $LaCl_3$ and other closely related lanthanide metal trichlorides have an ionic liquid structure which is dominated by the coulombic repulsion of the trivalent metal ions. Coordination numbers are relatively high and the local coordination structure is quite free to fluctuate, leading to mainly short-range order in the melt. The state of short-range order is in fact relatively poor for the monovalent anions. The nearest parallel is provided by liquid $SrCl_2$ among those molten salts which have been examined in detail by neutron diffraction to determine their partial structure factors.

This relatively simple type of molten salt structure evolves with decreasing R_M towards the more complex type which is illustrated by YCl_3. The first-neighbour

coordination is of octahedral type and the local structure is already sufficiently strengthened to allow a moderate degree of intermediate-range order from loose connectivity between octahedral-type structures. $DyCl_3$ may be expected to have a similar type of liquid structure.

Rapid changes in the topology of the melt occur within our model at still lower metal ion sizes, in the neighbourhood of $R_M \approx 1$ Å. The liquid is developing a very strong local structure of distorted tetrahedral type, with a parallel increase in the intermediate-range order. This topology is fully developed in $AlCl_3$ at the lower end of the range of R_M. Depending on the density of the liquid, its structure may be described as reflecting local charge compensation extending through connectivity into medium-range order or as formed by molecular-like units in strong mutual interaction. The intermolecular interactions are mainly multipolar in character and weaken rapidly with decreasing density, thus stabilizing the vapour phase. Quantitative predictions are more sensitive in this range to the detailed description of the interionic forces. In particular, for $AlCl_3$ our model has succeeded in yielding the Al_2Cl_6 dimers as the relevant molecular units, but even at moderately low density their shape is rather strongly distorted relative to what could be expected in the presence of halogen polarization and covalent contributions to the bonding.

Acknowledgments

We acknowledge sponsorship of this work by the Ministero dell'Università e della Ricerca Scientifica e Tecnologica of Italy through the Consorzio Interuniversitario Nazionale di Fisica della Materia. We are very grateful to Professor J Mochinaga for sending us the results of his x-ray diffraction studies of molten lanthanide metal chlorides. HT and ZA wish to thank Professor Abdus Salam, the International Atomic Energy Agency and UNESCO for hospitality at the International Centre for Theoretical Physics in Trieste.

References

[1] Tosi M P, Pastore G, Saboungi M-L and Price D L 1991 *Phys. Scr.* T **39** 367
[2] Akdeniz Z and Tosi M P 1992 *Proc. R. Soc.* A **437** 85
[3] Mochinaga J, Iwadate Y and Fukushima K 1991 *Mater. Sci. Forum* **73–5** 147
[4] Saboungi M-L, Price D L, Scamehorn C and Tosi M P 1991 *Europhys. Lett.* 15 283
[5] March N H and Tosi M P 1980 *Phys. Chem. Liquids* **10** 39
[6] Triolo R and Narten A H 1978 *J. Chem. Phys.* **69** 3159
[7] Pastore G, Akdeniz Z and Tosi M P 1991 *J. Phys.: Condens. Matter* **3** 8297
[8] Johnson E, Narten A H, Thiessen W E and Triolo R 1978 *Discuss. Faraday Soc.* **66** 287
[9] Abramo M C, Caccamo C, Pizzimenti G, Parrinello M and Tosi M P 1978 *J. Phys. C: Solid State Phys.* **9** L593
[10] Erbölükbas A, Akdeniz Z and Tosi M P 1992 *Nuovo Cimento* D **14** 87
[11] Busing R W 1970 *Trans. Am. Crystallogr. Assoc.* **6** 57
[12] Gillan M J 1979 *Mol. Phys.* **38** 1781
[13] Abernethy G M and Gillan M J 1980 *Mol. Phys.* **39** 839
[14] Hensel F 1979 *Adv. Phys.* **28** 555
[15] Moss S C and Price D L 1985 *Physics of Disordered Materials* ed D Adler, H Fritzsche and S R Ovshinsky (New York: Plenum) p 77
[16] Price D L, Moss S C, Reijers R, Saboungi M-L and Susman S 1989 *J. Phys.: Condens. Matter* **1** 1005
[17] McGreevy R L and Mitchell E W J 1982 *J. Phys. C: Solid State Phys.* **15** 5537